Journal of Institute of Science and Technology, 30(2), 25-33 (2025)
ISSN: 2467-9062 (print), e-ISSN: 2467-9240
https://doi.org/10.3126/jist.v30i2.82819

Research Article

STAR FORMATION RATE OF GALAXIES IN HCG7

Krishna Kumar Bhandari[1], Daya Nidhi Chhatkuli [2*], Amrit Sedain[1], Binil Aryal[1]
[1] Central Department of Physics, Tribhuvan University, Kathmandu, Nepal
[2]Tri-Chandra Multiple Campus, Tribhuvan University, Kathmandu, Nepal
[*]Correspondence*: chhatkulidn@gmail.com*

(Received:** August 7, 2025**; Revised**: November 1, 2025**; Accepted:** November 12, 2025**)

ABSTRACT

A small system of typically 4–10 galaxies that appear to be isolated from other galaxies and situated very close to one another on the sky leading to tidal distortions, gas stripping and star bursts is called a Hickson Compact Group (HCG). We present a spectroscopic analysis of four member galaxies of HCG 7: NGC 192, NGC 196, NGC 197, and NGC 201, using data from the Sloan Digital Sky Survey (SDSS) Data Release 12. Emission lines in the galaxy spectra are modeled with Gaussian profiles, and the Hα line is used to estimate Star Formation Rates (SFRs) and gas-phase metallicities. After extinction correction, we derive SFRs of 0.284 $M_{\odot}$/year, 0.222 $M_{\odot}$/year, and 0.034 $M_{\odot}$/year for the star-forming galaxies, NGC 192, NGC 201, and NGC 197, respectively with corresponding gas-phase metallicities (12 + log(O/H)) of 8.64 dex, 8.55 dex, and 8.56 dex. In contrast, NGC 196 shows no detectable Hα emission, consistent with a quiescent spectrum. The absence of a significant star-forming interstellar medium in NGC 196 may be attributable to environmental processes, with tidal stripping being the most probable quenching mechanism in the dense HCG 7 environment.

Keywords: Galaxy Merger, Hickson Compact Group, Metallicity, Star Formation Rate.

INTRODUCTION

Galaxies are fundamental building blocks of the universe in which billions of stars along with gas and dust, are gravitationally bound. According to their shape and size, there are different types of galaxies, such as elliptical, spiral, and irregular. Some galaxies consist predominantly of neutral gas, while others exhibit a very simple structure, composed only of ordinary stars without any distinct features (Karttunen, 2007).

Simulations have shown that galaxies in compact groups interact through gravitational tidal forces, implying that many of these systems are in a merging phase (Hickson *et al.*, 1997) and hence evolve faster than those in isolation. Compact groups often end in mergers and massive star formation takes place. Hickson Compact Groups (HCGs) are small, tightly bound collections of galaxies that are unusually close together in space compared to typical galaxy groupings. The Hickson Compact Group (HCG) catalog was first introduced by Hickson (1982) following the Palomar Observatory Sky (POS) survey, where one hundred compact groups were identified based on population, compactness, and isolation. These groups host galaxies of different morphologies, such as spiral, elliptical, and irregular, making them heterogeneous in composition (Hickson, 1993; Ribeiro *et al.*, 1998).

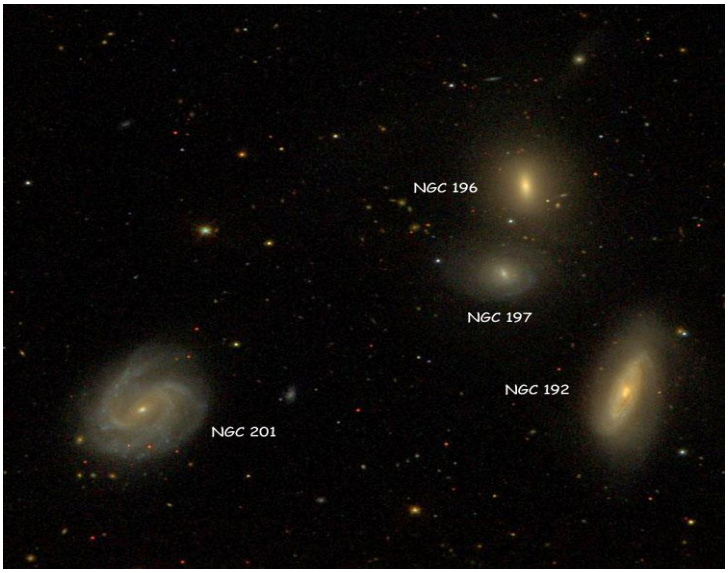

Figure 1. Hickson Compact Group 7 along with its four members NGC 192, NGC 196, NGC 197 and NGC 201.

[Source: https://cseligman.com/text/hickson.htm#hcg7]. NGC 192 is a barred spiral galaxy. NGC 196 is classified as an early-type spiral or lenticular galaxy (S0/a). NGC 201 is a late-type spiral galaxy (Sc). NGC 197 appears to be an irregular or dwarf spiral galaxy.

Hickson *et al.*, (1992), later refined the sample to 92 systems by removing groups with fewer than three confirmed members (Hickson, 1993). One major motivation for studying HCGs is to understand how strong interactions influence galaxy morphology and stellar content (Oliveira *et al*., 1994). Spectroscopic observations further help characterize the level of interaction, isolation, and internal activity within individual member galaxies (Diaferio *et al*., 1994). Figure 1 shows Hickson Compact Group 7 (HCG 7), that exhibit tidal features consistent with an ongoing merging process (Chhatkuli *et al.*, 2024). The largest member in this group is NGC 201. NGC 192 is relatively bright and gas-rich, exhibiting mild indications of tidal distortion. NGC 196 has a limited gas reservoir, suggesting a more evolved evolutionary stage**.** NGC 201 is abundant of neutral hydrogen (H I) and shows active star formation. In contrast**,** NGC 197 is comparatively faint but displaying possible tidal features and is evidence of ongoing star formation.

Star formation is a key tracer of galaxy evolution, as it reflects how stellar mass builds up over cosmic time (Chhatkuli *et al*., 2020). The star formation rate (SFR) is expressed in solar masses per year ($M_{\odot}$/year), indicating how much mass of the gas cloud is currently converted into stars per year. The SFR in a galaxy depends on several factors, including the availability of gas, dust, molecular clouds, and the influence of interactions with neighboring galaxies (Blom *et al.*, 2014).

Recent observational efforts have emphasized that HCGs exhibit a wide range of gas content and star-formation behavior, making them ideal laboratories to study environment-driven galaxy evolution. Deep H I surveys with Meer KAT have revealed that many HCGs undergo rapid transitions in their neutral gas reservoirs—progressing from complex tidal H I structures to states of substantial H I depletion—suggesting that gas removal and phase changes play a central role in quenching or modulating star formation (Ianjamasimanana *et al.*, 2025). X-ray and optical integral-field studies further show that shocks, hot intragroup gas, and collisional interactions can heat or displace cold gas and thereby suppress, or in some regions enhance, star formation activity. Consequently, recent work argues for galaxy-by-galaxy spectroscopic SFR diagnostics within HCGs to disentangle localized triggering from global quenching processes (O'Sullivan *et al*., 2025).

The primary objective of the study is to quantify the current level of star-forming activity within individual member galaxies of HCG 7 and to examine how galaxy–galaxy interactions within this compact environment influence star formation and gas-phase metallicities.

MATERIALS AND METHODS

Sample Selection

At first, we went through the HCG catalogue and made certain criteria for the selection. The main criterion for selection is that the member galaxies should have undergone a merging process.Then we followed the SDSS database and tried to collect all spectra of HCG galaxies. But, there were only some HCGs which have complete spectra. We selected only one compact group

HCG 7 containing emission features of galaxies, which have not been studied before. The HCG 7 located at R. A. of $00^h\ 36^m\ 50^s$ and Dec. of + 00 36′ 13″ has an angular diameter of 5.7 arc minutes of the circle containing the group (Hickson, 1982). The member galaxies HCG 192, HCG 201, HCG 197 and HCG 196 of HCG 7 are located at the redshift of 0.01393**,** 0.01461, 0.0137 and 0.01379 respectively. HCG 7 was selected as the focus of this study to enable a detailed, multi-wavelength analysis of star formation within a compact group environment. HCG 7 represents an ideal case study because it is relatively nearby, well-observed, and exhibits a diverse mix of galaxy morphologies, including both early- and late-type members. The group shows clear evidence of gravitational interactions, variable H I content, and ongoing star formation activity, making it a representative system for investigating how local dynamics influence galactic evolution.

Data Extraction and Processing

We retrieved FITS files of the galaxy by using SDSS DR 12 (Alam *et al*., 2015). We used ALADIN v2.5 for FITS spectral data extraction. On top of that, we use ORIGIN that has efficiency in handling multi-parameter Gaussian fitting, Graphing and analyzing. It makes easy to create different 2D and 3D graphs, like scatter plots, charts, as well as line graphs. ORIGIN was chosen for its integrated data management, curve-fitting, and high-quality plotting capabilities. ORIGIN provides robust nonlinear and spectral line-fitting tools, efficient statistical analysis, and customizable templates that ensure uniformity and reproducibility across all datasets. Its ability to consolidate raw data, fitting results, and graphical outputs within a single project file significantly streamlined the workflow and improved transparency in data handling. Therefore, Gaussian fitting and spectral visualization were performed using ORIGIN v8.0.

Spectral Analysis

We fitted Gaussian profiles on prominent emission and absorption lines to derive line centers, Full Width at Half Maximum (FWHM), and fluxes. By knowing the location of the center, we can understand the average value of the dataset. The height of the Gaussian curve gives the information regarding the intensity as well as the maximum frequency in the dataset. Moreover, with the help of the width of the Gaussian curve, we can understand the standard deviation, spread of data from the mean value.

Normal distribution is characterized by the coincidence of the mean, median, and mode, which signifies that the data are symmetrically distributed around the mean. If the distribution is not symmetric, those distributions have different mean, median and mode. This gives the skewness of the data. We calculated the spectroscopic contribution to the star formation rate (SFR). The spectra of HCG7 Galaxies NGC192, NGC196, NGC201 and NGC197 obtained from SDSS DR 12 are shown in the Figure 2. Prominent emission lines are observed above the continuum in the spectra of NGC 192, NGC 201, and NGC 197, indicating the presence of ionized gas and active star-forming regions which are the characteristics of emission-type galaxies**.** However, NGC 196 exhibits strong absorption lines in its spectrum, typical of an absorption-type galaxy dominated by an older stellar population with little or no ongoing star formation.

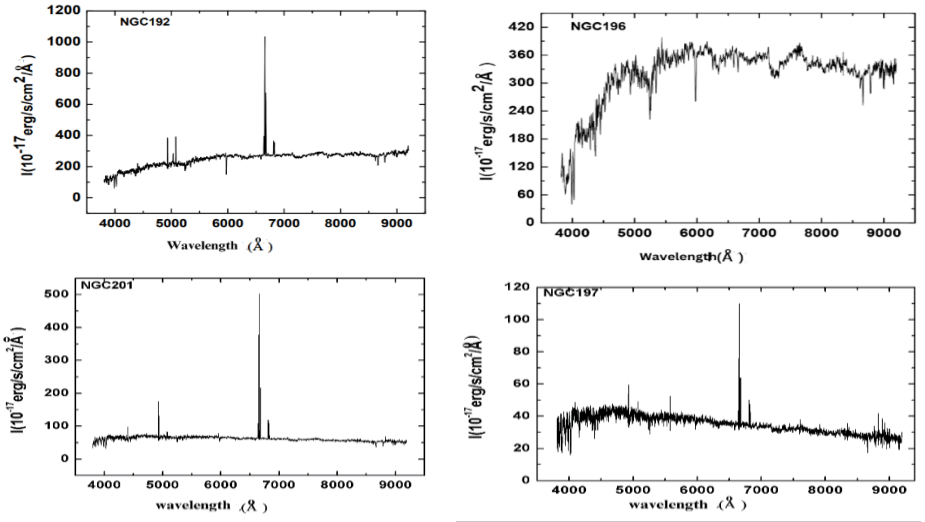

Figure 2. Spectra of Hickson Compact Group of Galaxy NGC192, NGC196, NGC201 and NGC197 obtained from SDSS DR 12 data. The galaxies NGC 192, NGC 201 and NGC 197 have strong emission lines above the continuum and hence are emission type galaxies while the galaxy NGC 196 is absorption type as it has strong absorption lines below the continuum.

Star Formation Rate (SFR)

The star formation rate (SFR) of galaxies provides insights into their evolutionary stages and star-formation histories As shown in Figure 3, the global Schmidt law (1959) expresses how the surface density of star formation correlates with the surface density of gas. The upper pair containing solid squares indicates circumnuclear starbursts. The solid dark circle infers the normal spirals, and open circles represent the star formation rates as well as gas densities in the central region of normal disks. This demonstrates that star formation rate is directly proportional to the density of galaxies. Therefore, star formation occurs in giant molecular clouds (Kennicutt, 1998).

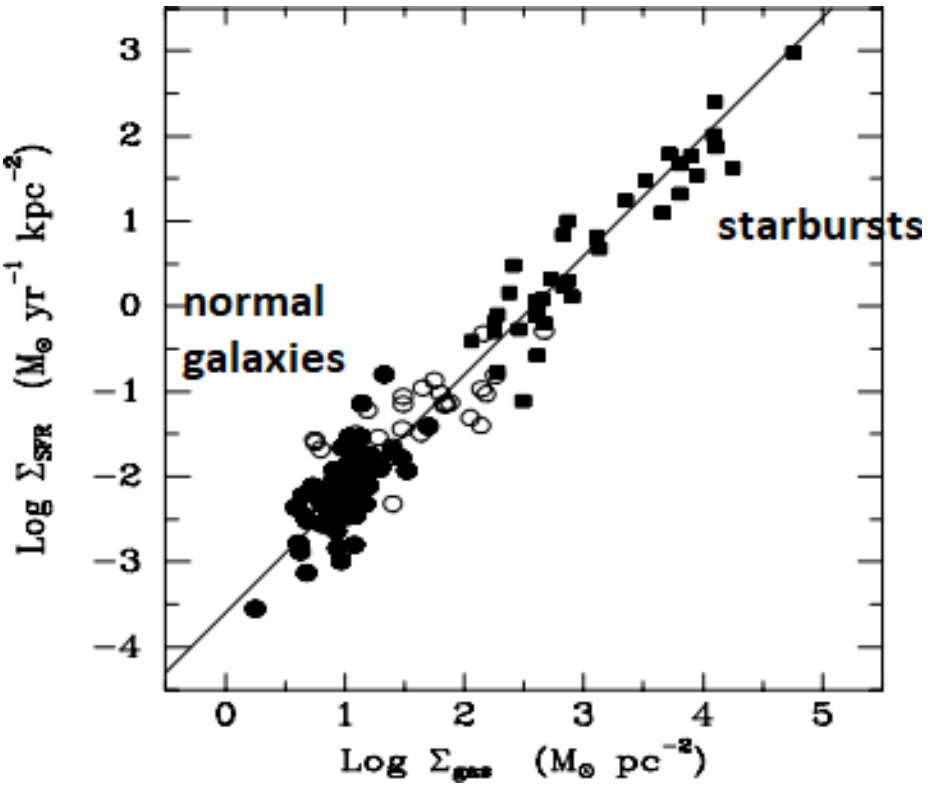

Figure 3. Surface density of star formation as a function of gas surface density. (Source: Schmidt, 1959).

Emission line plays a crucial role to estimate the SFR. Mostly, astronomers use H_α and OIII as an indicator of SFRs. It can be determined from the H_α, H_β, OIII and UV emission lines. SFR of a galaxy can be calculated by using the relation by Kennicutt (1998) as

$$SFR(M_\odot/yr = L(H\alpha) \times 7.9 \times 10^{-42}\ erg/sec \quad (1)$$

Here, L(H_α) represents total fitted flux density obtained from the Gaussian fit of broad characteristic lines.

Metallicity

The metallicity is used to describe the mass fraction of elements heavier than helium in the galaxy. Old Stars can have metal-rich or poor that depends on whether they reside in a passive galaxy or in star-forming galaxy (Gallazzi *et al*., 2005). When an atom in a higher energy state moves down to a lower energy state, it will emit a photon having a characteristic wavelength. There are several possible transitions between energy states and several possible wavelengths of electromagnetic radiation that can be emitted for a particular element. Similarly, when light passes through the cold clouds, it absorbs photons at a particular frequency as a result of jumping electrons to higher energy levels. This shows that the spectrum of a star will have a series of peaks with corresponding emission lines of particular elements and a series of troughs which correspond to absorption lines.

The gas-phase metallicity can be calculated by using the following relation (Marino *et al*., 2013).

$$12 + log\ (O/H) = 8.743 + 0.462 \times log\ (NII/H\alpha)\ (2)$$

Uncertainties in metallicity were computed by propagating the flux measurement errors of NII and Hα lines.

Redshift Correction

Observed wavelengths are redshifted because of Hubble recessional velocity of the galaxy. It can be corrected by using this relation:

$$\lambda_{corrected} = \frac{\lambda_{Observed}}{z+1} \qquad (3)$$

Equation (3) gives the corrected values of wavelength, where z is the redshift of the galaxy and $\lambda_{Observed}$ is the observed value of wavelength.

Extinction Correction

Balmer decrement line ratio is c = Hα/Hβ. Theoretical value of $c_0 = 2.86$ for an electron temperature of 10^4 K. Now, extinction coefficient E (B − V) = 1.97× log (c/c_0). Now, extinction A (Hα) = 2.45 E (B–V).

Again, we have

$$A(H\alpha) = -2.5\ log\ (F(H\alpha)obs/F(H\alpha)em)\ (4)$$

Using the value of observed flux from equation (4), SFR can be calculated by using equation (1).

RESULTS AND DISCUSSION

SDSS Spectroscopy

We performed Gaussian fittings on nine, six and five emission lines of NGC 192, NGC 201 and NGC 197 respectively. Emission lines often follow a Gaussian shape due to the combined effects of thermal motions, turbulent gas motions, and instrumental broadening. By fitting a Gaussian function, we can accurately extract key parameters such as wavelength, Line flux, Full Width at Half Maximum (FWHM), Peak intensity and so on. In Figure 4, the Gaussian fits of the strongest H_α emission lines of the galaxies NGC 192, NGC 201 and NGC 197, respectively are shown. The plot shows the observed line profiles and best-fit Gaussian models. The solid curve represents the Gaussian fit. Solid circles with statistical standard error bars represent the observed SDSS data. The standard error of deviation is used for the statistical error bars.

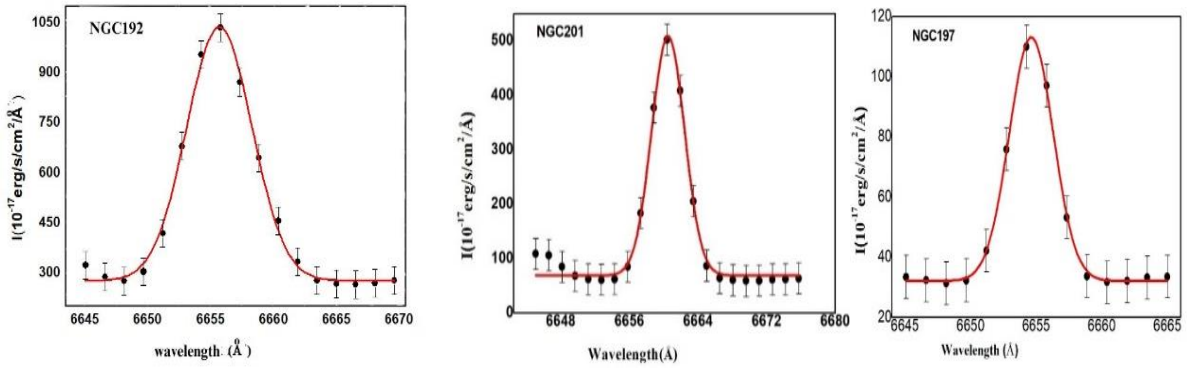

Figure 4. Characteristic peaks of the H_α emission lines in the spectra of NGC192, NGC201 and NGC197 respectively. These wavelengths are redshifted because of Hubble recessional velocity of these galaxies. The error bars represent ±1σ standard error of the deviation.

Gaussian parameters obtained after Gaussian fitting on different emission lines of the galaxies NGC 192, NGC 201 and NGC 197 are presented in the Tables 1, 2 and 3 respectively. In each table, the first, second, third, fourth and fifth columns represent serial number, redshift corrected wavelength, peak intensity corresponding to peak wavelength, corresponding elements responsible for emission of the respective lines, and area of the Gaussian curve respectively. The sixth, seventh, eighth and ninth columns represent height of the Gaussian curve, offset, coefficient of regression and full width at half maximum respectively.

The flux value for the Hα emission line is used to estimate the star formation rate (SFR) of the respective galaxies. From Tables 1, 2, and 3, we find that the maximum intensities for NGC 192, NGC 201, and NGC 197 are (1035, 502, and 110) × 10^{-17} erg/s/cm^2/Å, occurring at wavelengths 6564 Å. These peaks correspond to the Hα emission in each galaxy.

Table 1. The Gaussian parameters of nine prominent emission lines of the galaxy NGC 192.

S.N.	Corrected Wavelength (Å)	I (×10^{-17}erg/s/cm^2/Å)	Elements	Area (erg/s/cm^2/Å)	Height (erg/s/cm^2/Å)	Offset (Å)	R^2	FWHM (Å)
1	3969	73	NIII	-943.9	−69.6	-1	0.972	12.7
2	4341	220	H_γ	167.8	53.5	+0.2	0.896	2.9
3	4862	385	H_β	859.4	195.0	-0.3	0.990	4.2
4	5008	391	OIII	869.5	184.0	-0.5	0.978	4.4
5	6550	394	NII	739.3	119.0	-1	0.958	5.8
6	6564	1035	H_α	4948.2	760.0	+0.1	0.992	6.1
7	6585	673	NII	2888.8	403.0	+0.1	0.998	6.7
8	6718	365	SII	614.6	91.7	+0.3	0.970	6.3
9	6733	356	SII	657.4	86.4	-0.005	0.983	7.2

Table 2. The Gaussian fit parameters for six prominent emission lines of the galaxy NGC 201.

S.N.	Corrected Wavelength (Å)	I (×10^{-17}erg/s/cm^2/Å)	Elements	Area (erg/s/cm^2/Å)	Height (erg/s/cm^2/Å)	Offset (Å)	R^2	FWHM (Å)
1	4342	98	H_γ	122.9	45.26	−0.5	0.930	2.6
2	4863	175	H_β	427.6	121.9	+0.3	0.994	3.1
3	6564	502	H_α	2117.8	439.8	−0.1	0.986	4.5
4	6585	217	NII	810.0	159.7	+0.4	0.999	4.8
5	6718	119	SII	303.3	60.93	+0.7	0.998	4.7
6	6733	109	SII	233.1	48.09	+0.1	0.998	4.6

The emission lines H_β, H_α, NII_{6585}, SII_{6718} and SII_{6733} are common in all three emission galaxies. Additional $NIII_{3969}$, H_γ, $OIII_{5008}$, and NII_{6550} lines are found in the spectrum of NGC 192. The regression coefficient of all lines is more than 93 %. This means that the observed data is well fitted with Gaussian distribution.

A negative value for the Gaussian area and peak height is obtained for the [O III] line in NGC 192**.** A negative Gaussian area typically indicates that the feature behaves as an absorption line or that the local continuum has been overestimated during the fitting process. Such outcomes generally arise when the emission feature is weak, influenced by noise, or when the baseline is not modeled accurately.

Across all tables, the Gaussian fits show both positive and negative offsets for different emission lines, indicating fluctuations in the continuum baseline around the spectral features. In Gaussian fitting of spectral lines, the offset refers to the baseline value (the continuum level) around which the Gaussian curve is centered. In practice, a positive offset represents a normal positive continuum level, whereas a negative offset generally results from continuum over-subtraction or noise during the fitting process.

The FWHM values obtained from Gaussian fitting represent the velocity dispersion of the ionized gas in the galaxies. Higher FWHM values indicate fast-moving or turbulent gas, while lower values correspond to quiescent star-forming regions. Thus, variation in FWHM across different emission lines provides insight into the kinematic state and physical conditions of the emitting regions. The FWHM values lie in the range **(**2.9–12.7) Å for NGC 192**, (**2.6–4.8) Å for NGC 201, and **(**2.5–4.3) Å for NGC 197, with NGC 192 exhibiting significantly broader line widths, suggestive of stronger kinematic disturbance relative to the other group members. NGC 192 stands out as the most kinematically disturbed system and is the most likely candidate for strong interaction-driven effects (e.g., shocks, outflows, or AGN-related broad components). NGC 201 and NGC 197 appear to host predominantly star-formation–dominated ionized gas with comparatively modest kinematic disturbance.

Table 3. Gaussian fitting results for five prominent emission lines of NGC 197.

S.N.	Corrected Wavelength (Å)	I ($\times 10^{-17}$ erg/s/cm^2/Å)	Elements	Area (erg/s/cm^2/Å)	Height erg/s/cm^2/Å	Offset (Å)	R^2	FWHM (Å)
1	4863	60	H_β	70.3	26.8	+0.4	0.982	2.5
2	6564	110	H_α	339.8	81	−0.4	0.998	3.9
3	6585	64	NII	134.6	31.8	+0.3	0.992	4.0
4	6718	50	SII	74.3	16.8	+0.4	0.984	4.2
5	6733	48	SII	59.0	13.2	+0.1	0.951	4.3

These tables reflect that most of the intensity peaks are above the average value of intensity, and only a few of them are below the average value of intensity. This means that the spectra of these galaxies are emission-type. Those peaks that are below the continuum represent the absorption peaks of the galaxy. Most of the peaks of NGC196 are below the continuum level, which means the spectra of NGC196 is absorption type. So, there is no emission of the H_α line in NGC196, and we do not tabulate the data of this galaxy.

Star Formation Rate

By using redshift velocity relation, the radial velocities of the galaxies NGC 192, NGC 201 and NGC 197 are calculated to be (4.15, 4.35 and 4.08) $\times 10^6$ m/s respectively. The Hubble distance *D* of these galaxies are obtained by using Hubble's law ($V = H_0D$) for a given redshift (Kennicutt, 1998). Therefore, D = (59.28, 62.14 and 58.29) Mpc for NGC192, NGC201 and NGC197, respectively. The radius is calculated by using the relation $R = D \times 3.08 \times 10^{24}$ cm. The SFRs of NGC 192**,** NGC 201, and NGC 197, calculated by using Equation (1) before extinction correction, are 0.164 $M_{\odot}$/year, 0.077 $M_{\odot}$/year, and 0.0109 $M_{\odot}$/year, respectively. After applying extinction correction using Equation (4) and (1), the SFRs increase to 0.284 $M_{\odot}$/year, 0.222 $M_{\odot}$/year, and 0.0340 $M_{\odot}$/year, respectively. This indicates that the SFR values after correction are more than double the uncorrected values, highlighting that the intrinsic flux of these galaxies is significantly higher than what is observed**,** due to absorption and scattering by dust. Moreover, the SFR appears to be highest in NGC 192 and lowest in NGC 197 among the three actively star-forming galaxies, suggesting that NGC 192 is experiencing more vigorous star-forming activity, possibly triggered by interactions within the group. In contrast, NGC 196 shows little to no star formation and appears largely quiescent, consistent with its classification as an early-type or lenticular galaxy with depleted gas content.

Gas-phase Metallicity

The gas-phase metallicities of NGC 192**,** NGC 201, and NGC 197, calculated using Equation (2), are 8.635 dex**,** 8.550 dex**,** and 8.557 dex, respectively. These relatively high values indicate that all three galaxies have undergone significant chemical enrichment, consistent with ongoing or past star formation. NGC 192**,** which also shows the highest star formation rate, has the highest oxygen abundance, suggesting that its enhanced star-forming activity may have contributed to a greater build-up of metals in its interstellar medium. Conversely, NGC 201 and NGC 197 have slightly lower metallicities, reflecting somewhat less active star formation or possible dilution from gas inflows. The combination of similar metallicities and varying SFRs suggests that interactions within the compact group may be modulating star formation efficiency, with gravitational encounters triggering bursts in some galaxies while others, such as NGC 197, remain less active. Overall, these trends highlight the influence of the compact group environment on both chemical enrichment and star-forming activity.

Using the same spectroscopic method, Chhatkuli *et al.* (2024) calculated the SFR of a low redshift (z = 0.0059) interacting galaxy Mrk 1481, to be 0.0055 $M_{\odot}$/yr. We see that the three members of HCG7 (NGC192, NGC201 and HCG197) have higher values of SFR as compared to Mrk 1481. This is evident that H_α lines in NGC192, NGC201 and NGC197 are more prominent as compared to Mrk 1481 and are the younger galaxies.

Similarly, the results of Paudel *et al*. (2021) for dwarf galaxies (SDSSJ222726.64+120539.8 and SDSSJ162753.47+482529.3) were found to be 0.010 $M_{\odot}$/yr and 0.016 $M_{\odot}$/yr respectively, which indicate that members of HCG7, have higher SFR compared to these two dwarf galaxies. Thus, HCG7 members reflect the strong influence of the compact group environment. Gravitational interaction and tidal forces may trigger gas inflows, enhancing the star formation

rate. In contrast, Dwarfs often have lower gas content in an isolated environment.

The SFRs obtained for the HCG 7 galaxies are consistent with the modest levels typically observed in compact groups. Tzanavaris *et al.* (2010) reported SFRs in HCG systems that generally remain below ~1 $M_{\odot}$/yr, while Martínez-Badénes *et al.* (2012) similarly found that spiral members of compact groups often exhibit SFRs comparable to isolated field galaxies rather than undergoing strong starburst activity. Our results, therefore, indicate that HCG 7 follows this broader trend, displaying moderate star-formation activity. Additionally, the variation in SFR among the HCG 7 members ~ (0.03–0.28) $M_{\odot}$/yr reflects the diversity commonly seen within compact groups, suggesting that environmental effects act in a non-uniform manner—enhancing star formation in some galaxies while leaving others relatively quiescent.

CONCLUSIONS

In this study, we conducted a spectroscopic investigation of the galaxies in HCG 7 to examine their emission-line properties, SFRs, dust extinction effects, and gas-phase metallicity, providing insight into the evolutionary processes operating in compact galaxy environments. Gaussian fitting of prominent emission lines provided reliable measurements of Hα flux, which served as the primary tracer of SFR for the star-forming galaxies in the group environment. We estimated SFR of the galaxies NGC 192, NGC 201, and NGC 197. Extinction correction significantly increased the SFR estimates, demonstrating that dust plays a major role in attenuating observed Hα flux in compact-group galaxies. We found that after extinction correction, the star formation rate of NGC 192 dominates the other two, NGC 201 and NGC 197. These variation in star formation result suggests that the star formation environment in a compact group of galaxies is affected by various factors, such as gravitational interaction, tidal interaction or gas depletion. Among the four members of HCG 7, only three show an active star formation environment. However, HGC 196 remains quiescent. This indicates that the gases of NGC 196 might have been expelled through tidal force. The gas-phase oxygen abundances (12 + log(O/H)), derived using the NII calibration, indicate near-solar metallicities, consistent with mature stellar populations and previous interaction events. For future studies with deeper spectroscopy, multi-wavelength observations (UV, IR) or comparison with simulations will help to understand galaxy evolution over time.

ACKNOWLEDGMENTS

This study is based on the archival images and spectra from the Sloan Digital Sky Survey (*http://www:sdss.org/collaboration/credits.html*).

AUTHOR CONTRIBUTIONS

Conceptualization: KKB, BA, DNC; Investigation: KKB, AS, DNC; Methodology: KKB, DNC; Data curation: KKB, AS; Data analysis: KKB, DNC, AS; Writing – original draft: KKB; Writing - review and editing: KKB, BA, DNC.

CONFLICT OF INTEREST

The authors do not have any conflict of interest pertinent to this work.

ETHICAL STATEMENT

This article presents our original work and has not been published or submitted elsewhere.

DATA AVAILABILITY STATEMENT

The data that support the findings of this study are openly available in SDSS. The SDSS website can be accessed at www.sdss.org.

REFERENCES

Alam, S., Albareti, F. D., Allende Prieto, C., Anders, F., Anderson, S. F., Anderton, T., ... & York, D. G. (2015). The Eleventh and Twelfth Data Releases of the Sloan Digital Sky Survey: Final data from SDSS-III. *The Astrophysical Journal Supplement Series*, *219*(1), 12. https://doi.org/10.1088/0067-0049/219/1/12.

Blom, C., Forbes, D. A., Foster, C. Romanowsky, A. J., & Brodie, J. P. (2014). The SLUGGS Survey: new evidence for a tidal interaction between the early-type galaxies NGC 4365 and NGC 4342, *Monthly Notices of the Royal Astronomical Society*, *439*, 2420–2431.

Chhatkuli, D. N., Paudel, S., & Aryal, B. (2020). Study of Star Formation Rate and Metallicity of an Interacting Dwarf Galaxy NGC 2604. *Journal of Institute of Science and Technology*, *25*(2), 55-60.

Chhatkuli, D. N., Paudel, S., Sedain, A., & Aryal, B. (2024). Dwarf galaxy merger-induced star formation rate: A case study of Mrk 1481. *Bibechana*, *21*(2), 95-102.

Diaferio, A., Geller, M. J., & Ramella, M. (1994). The Formation of Compact Groups of Galaxies. I. Optical Properties. *The Astronomical Journal*, *107*, 868-885.

Gallazzi, A., Charlot, S., Brinchmann, J., White, S. D. M., & Tremonti, C. A. (2005). The ages and metallicities of galaxies in the local universe.

Monthly Notices of the Royal Astronomical Society, 362, 41-58.

Hickson, P. (1993). Atlas of Compact Groups of Galaxies. *Astrophysical Letters and Communications,* 29, 1.

Hickson, P. (1997). Compact groups of galaxies. *Annual Review of Astronomy and Astrophysics, 35*, 357-388.

Hickson, P., Oliveira C. M. D., C., Huchra, J. P., & Palumbo, G. G. (1992). Dynamical properties of compact groups of galaxies. *The Astrophysical Journal, 399*, 353-367.

Hickson, P. (1982). Systematic properties of compact groups of galaxies. *The Astrophysical Journal, 255*, 382-391. https://cseligman.com/tex/hickson.htm#hcg7.

Ianjamasimanana, R., Verdes-Montenegro, L., Sorgho, A., Hess, K. M., Jones, M. G., Cannon, J. M., ... & Smirnov, O. M. (2025). MeerKAT view of Hickson Compact Groups-I. Data description and release. *Astronomy & Astrophysics*, *696*, A176.

Karttunen, H., Kröger, P., Poutanen, M., & Donner, K. J. (2007). *Fundamental astronomy* (5th ed.). Springer.

Kennicutt, R. C. (1998). Star formation in galaxies along the Hubble sequence. *Annual Review of Astronomy and Astrophysics, 36*, 189-232.

Martínez-Badénes, V., Lisenfeld, U., Espada, D., Verdes-Montenegro, L., García-Burillo, S., León, S., Sulentic, J., & Yun, M. S. (2012). Molecular gas content and star formation rate in Hickson Compact Groups: Enhanced or deficient? *Astronomy & Astrophysics, 540*, A96. https://doi.org/10.1051/0004-6361/201117281.

Oliveira, C. M. D., & Hickson, P. (1994). Morphology of Galaxies in Compact Groups. *The Astrophysical Journal, 427*, 684-695.

Ribeiro, A. L. B. and Carvalho, R. R. D., Capelato, H. V., & Zepf, S. E. (1998). Structural and dynamical analysis of the Hickson compact groups. *The Astrophysical Journal, 497*, 72-82.

Schmidt, M. (1959). The rate of star formation. *The Astrophysical Journal, 129*, 243. doi: 10.1086/146614.

Tzanavaris, P., Hornschemeier, A. E., Gallagher, S. C., Johnson, K. E., Gronwall, C., Immler, S., Reines, A. E., Hoversten, E., & Charlton, J. C. (2010). Ultraviolet+Infrared star formation rates: Hickson Compact Groups with Swift and Spitzer. *The Astrophysical Journal, 716*(1), 556-573. https://doi.org/10.1088/0004-637X/716/1/556.

1